

Paleorainfall Reconstructions from Pedogenic Magnetic Susceptibility Variations in the Chinese Loess and Paleosols

BARBARA A. MAHER

School of Environmental Sciences, University of East Anglia, Norwich NR4 7TJ

AND

ROY THOMPSON

Department of Geology and Geophysics, University of Edinburgh, EH9 3JW, United Kingdom

Received March 9, 1995

The rock magnetic properties of the Chinese loess and paleosols constitute a unique and sensitive record of East Asian paleoclimate through the Quaternary Period. Systematic variations in the concentration and grain size of the magnetic minerals in these sediments have produced systematic variations in the magnetic susceptibility signal, which can be easily and rapidly measured at many sites across the Loess Plateau. Variations in many other rock magnetic properties can be used to identify the key shifts in ferrimagnetic grain size, but magnetic susceptibility alone is sufficiently sensitive to record stadial and interstadial climate stages, as well as glaciations and interglaciations. Past changes in rainfall and monsoon activity for this region are reconstructed from the susceptibility variations. The susceptibility record is calibrated using the modern relationship between rainfall and pedogenic susceptibility on the Loess Plateau. Our rainfall reconstructions identify enhanced summer monsoonal activity in the Chinese Loess Plateau region in the early Holocene and the last interglaciation. In the presently semiarid western area of the plateau, annual precipitation in interglacial times was up to 80% higher than at present; in the more humid southern and eastern areas, values were up to 20% higher than today's levels. During the last glaciation, precipitation decreased across the entire plateau, typically by ~25%. The relationship between pedogenic susceptibility, climate, and weathering age was examined over the Northern Hemisphere temperate zone and the observed positive correlation between rainfall and susceptibility indicates that climate, rather than soil age, is the predominant factor that controls pedogenic susceptibility enhancement in loess soils. ©1995 University of Washington.

INTRODUCTION

Variations in the magnetic susceptibility records of the Chinese loess and paleosols have been interpreted as proxy indicators of Quaternary climate change. These variations in susceptibility, which reflect changes in the concentration and magnetic grain size of the iron oxides in these sediments, have been used to make qualitative assessment of climate change in this region. Higher susceptibility values, associated with the paleosol horizons, are interpreted as indicating warmer and

more humid phases; lower values from the less-weathered loess layers represent cooler and drier phases (e.g., Heller and Liu, 1986). More recently, we have made quantitative reconstruction of paleoprecipitation patterns across the Loess Plateau, for the last glacial/interglacial cycle, based on a climofunction calculated from the relationship between the *in situ* pedogenic susceptibility of some modern Chinese soils and present climate (Maher *et al.*, 1994). This calculated climofunction calibrates susceptibility against rainfall and hence enables paleorainfall reconstructions to be made from the paleosusceptibility variations. Here, we extend our paleoclimatic reconstructions to the last 1.1 myr at a central Loess Plateau site (Xifeng) and examine the spatial pattern of monsoonal rainfall for time slices through the last glacial/interglacial cycle.

A key step in using any soil property for quantitative reconstruction of paleoclimate is to establish its behavior with time. Some soil properties develop in a linear fashion and hence are mainly dependent on weathering duration; some evolve rapidly toward a near-steady-state equilibrium, and hence reflect ambient soil-forming conditions. Some properties may develop at a low initial rate and then an increasing rate with time. In the case of a soil property displaying a linear rate of development, that property has potential as a long-term (>10⁴ yr) chronometer (e.g., Pavich *et al.*, 1986). Alternatively, where a soil property rapidly changes and reaches "saturation," within hundreds to a few thousand years (e.g., rapid changes in surface pH), it could be used only as a short-term chronometer or as a rapidly responding indicator of the soil-forming climate. Furthermore, if such a rapidly evolving soil property reaches near-steady state in a soil profile which is subsequently buried to form a paleosol, a record of the past environment will be encapsulated and preserved as a natural archive.

In order to use the specific soil property, pedogenic susceptibility, as a paleoclimate recorder for the Chinese loess and paleosols, it is essential to establish that it is a property reaching near-steady state within a few thousand years, and hence one providing a "snapshot" of soil-forming conditions for every paleosol that has had this minimum exposure time to

weathering. A continually developing soil property cannot be used in this way, as it is also dependent on the duration of exposure to weathering (and, by inference, on sediment accumulation rate). Singer *et al.* (1992), on the basis of chronosequence studies on some Californian soils, suggest pedogenic susceptibility develops linearly with time. Here, we present evidence that suggests rapid development of pedogenic susceptibility, especially on loess parent materials.

SUSCEPTIBILITY VARIATIONS IN THE CHINESE LOESS PLATEAU

The initial magnetic susceptibility of a sediment, its "magnetizability," is quickly and easily measured by applying a small external ac or dc field (H), measuring its magnetic response (M), and calculating the ratio, M/H . Ferrimagnetic iron oxides like magnetite (Fe_3O_4) and maghemite ($\gamma\text{Fe}_2\text{O}_3$) have much higher susceptibilities ($\sim 1000\times$ higher) than the weakly magnetic oxides, hematite ($\alpha\text{Fe}_2\text{O}_3$), goethite (αFeOOH), and the paramagnetic iron-rich silicates or clays. For samples containing ferrimagnetic minerals of nonvarying grain size, the value of susceptibility is a reliable indicator of the samples' magnetic content. However, where ultrafine ferrimagnetic particles ($\leq 0.03 \mu\text{m}$) are present, these can contribute $\sim 10\times$ the susceptibility of the larger ferrimagnetic particles.

In loess and paleosol samples from the Chinese Loess Plateau, the soil samples have susceptibility values 2–5 \times higher than the less-weathered loess layers (Fig. 1b). Applying a range of additional rock magnetic analyses (e.g., Evans and Heller,

1994; Maher and Thompson, 1991) and independent analysis by electron microscopy and Mössbauer analysis (e.g., Maher and Thompson, 1992; Vandenburghe *et al.*, 1992), it has been shown that the main cause of these susceptibility variations is an increased concentration of ultrafine ferrimagnetic grains in the paleosols. That is, although there are larger ($> 1 \mu\text{m}$) detrital grains of magnetite, and some hematite grains, in the parent loess, these contribute a "background" susceptibility value (averaging $\sim 28 \times 10^{-8} \text{ m}^3 \text{ kg}^{-1}$). The *in situ* precipitation of ultrafine ferrimagnetic grains, during and as a response to soil formation, dominates the susceptibility signal. Because of their large surface area, these ultrafine grains are prone to surface oxidation to maghemite. A small proportion ($< 1\%$) of these ultrafine grains are formed intracellularly by magnetotactic bacteria (Fig. 2a); most ($> 99\%$) appear to be formed by inorganic precipitation (Fig. 2b), probably mediated by production of Fe^{2+} by iron-reducing bacteria. These latter bacteria function during periods of wetness and anoxia within the soil microenvironment. They decompose organic matter, using iron oxides as the electron acceptor for their metabolism. They release the Fe^{2+} thus formed into the extracellular environment; this provides the $\text{Fe}^{2+}/\text{Fe}^{3+}$ mix that induces the inorganic precipitation of magnetite (Taylor *et al.*, 1987). Such precipitation of magnetite is favored in near-neutral pH conditions. As there is no biological control over the extracellular, chemical precipitation of the mixed $\text{Fe}^{2+}/\text{Fe}^{3+}$ oxide, magnetite, the resultant grain size is determined by the rate of oxidation (as the soil dries out), the pH, and the Fe concentration (Taylor *et al.*, 1987). Excessively wet conditions, as in a waterlogged soil, favor Fe reduction and dissolution of magnetic iron oxides.

The pedogenic magnetic grainsize distribution thus dominantly reflects environmental conditions favoring the action of the iron-reducing bacteria and consistently comprises a mix of ultrafine ($\leq 0.03 \mu\text{m}$) and fine ($\sim 0.03\text{--}0.05 \mu\text{m}$) grains (Fig. 2b). Hundreds of such magnetic grains can be formed via the action of one iron-reducing bacterium (Lovley *et al.*, 1987). Magnetotactic bacteria, on the other hand, produce biologically controlled magnetic grains of fine size ($\sim 0.03\text{--}0.05 \mu\text{m}$). These grains have susceptibilities somewhat lower than those of both the *in situ* ultrafine grains and the detrital large ($\geq 1 \mu\text{m}$) grains.

In summary, ultrafine grains of magnetite are efficiently produced in a soil which is well-drained but alternately wetted (Fe^{2+} produced) and dried ($\text{Fe}^{2+}/\text{Fe}^{3+}$ oxide precipitated), with a supply of organic matter and Fe, and under near-neutral pH conditions. We would predict that, given sufficient iron and organic matter, a well-drained soil will form higher concentrations of ultrafine magnetite/maghemite in regions of higher rainfall (i.e., the greater the number of wetting/drying cycles in the soil microenvironment, the greater the pedogenic susceptibility). Conversely, the drier the climate, the more oxidation of iron proceeds and the more oxic forms of iron, such as goethite and hematite, accumulate. Given the minimum period of soil formation (with weathering release of Fe and colonization by vegetation and soil fauna), the subsequent balance be-

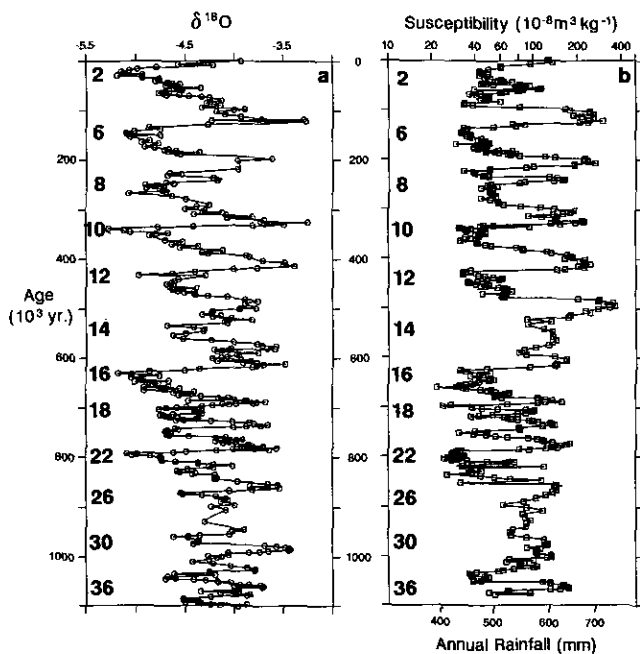


FIG. 1. (a) Oxygen isotope record from Site 677, from Raymo *et al.* (1990). (Note that a revised chronology for Site 677 has been suggested by Tiedemann and Sarnthein, 1994.) (b) Magnetic susceptibility (Liu *et al.*, 1992) and reconstructed rainfall values for Xifeng, central Loess Plateau, for the last 1.1 myr.

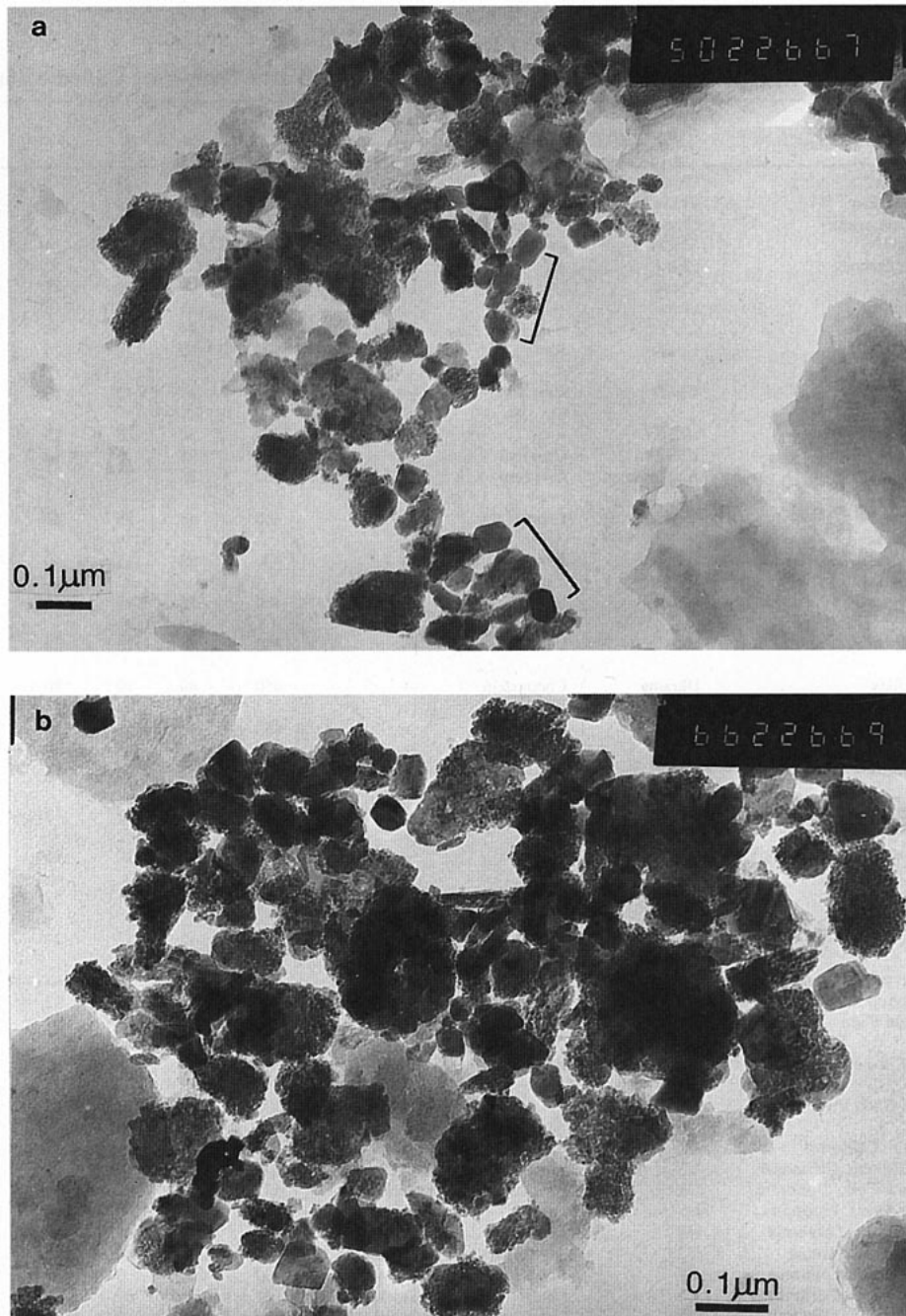


FIG. 2. Transmission electron micrographs of ultrafine ferrimagnetic particles extracted from paleosol S₅; (a) produced by magnetotactic bacteria, (b) produced by inorganic precipitation via iron reduction by iron-reducing bacteria.

tween oxidation and reduction of iron will determine by dynamic equilibrium the maximum pedogenic susceptibility of a soil.

CLIMATE RECONSTRUCTION

If the pedogenic susceptibility of the Chinese loess and paleosols is a rapidly formed soil property, we can use the preserved paleosusceptibility values directly to reconstruct paleorainfall. We can discount weathering duration and therefore

avoid having to use sediment accumulation rates to calculate the fluxes of susceptibility as other workers (e.g., Heller *et al.*, 1993) are forced to do. We can thus avoid the critical problems of assigning age models and subsequently calculating accumulation rates (Thompson and Maher, in press). In this study, we use the calibration obtained from the relationship between modern rainfall and the pedogenic susceptibility of young soils on the Loess Plateau (Maher *et al.*, 1994) to reconstruct paleorainfall for time slices within the last glacial/interglacial cycle, and for the last 1.1 myr at Xifeng, in the central Loess Plateau

TABLE 1
Magnetic Susceptibility Enhancement in the Temperate and Warm Temperate Climatic Zones

Latitude (°N)	Longitude (°W)	Locality	Country	FAO soil type	Parent material	Rainfall (mm/yr)	χ^B	χ^C	$\chi^{(B-C)}$	Reference
37.2	104.1	Jingtai	China	Xerosol	Loess	321	17	13	4	Maher <i>et al.</i> (1994)
38.0	109.1	Hengshan	China	—	Loess	445	26	14	12	Maher <i>et al.</i> (1994)
35.8	104.1	Xinglongshan	China	Cambisol	Loess	445	39	19	20	Maher <i>et al.</i> (1994)
39.1	110.7	Fugu	China	—	Loess	447	60	46	14	Maher <i>et al.</i> (1994)
35.13	109.9	Chengcheng	China	—	Loess	560	92	34	58	Maher <i>et al.</i> (1994)
34.8	105.7	Qinan	China	—	Loess	582	75	30	45	Maher <i>et al.</i> (1994)
34.5	109.5	Weinan	China	—	Loess	630	145	35	110	Maher <i>et al.</i> (1994)
27.8	99.7	Zhongdian	China	—	Limestone	700	49	0	49	Maher (unpub.)
46	42	Rostov	USSR	Kastanozem	—	500	32	18	14	Vadyunina and Smirnov (1976)
54.1	37.6	Tula abatis	USSR	Greyzem	—	550	20	10	10	Vadyunina and Smirnov (1976)
57.5	52.5	Udmurt	USSR	—	—	500	30	5	25	Lukshin <i>et al.</i> (1968)
57.5	52.5	Udmurt	USSR	Greyzem	—	500	21	5	16	Lukshin <i>et al.</i> (1968)
38.8	48.9	Lenkoran	Azerbaijan	Greyzem	—	300	26	10	16	Vadyunina and Babanin (1972)
47.0	37.5	Zhdanov	Ukraine	Chernozem	—	400	48	25	23	Vadyunina and Babanin (1972)
46.5	33.9	Askaniya	Ukraine	Kastanozem	—	400	55	15	40	Vadyunina and Babanin (1972)
47.5	44.3	Yergeni Hills	USSR	Solonetz	—	400	55	15	40	Vadyunina and Babanin (1972)
49.9	37.4	Shipov	Ukraine	Greyzem	—	450	48	25	23	Vadyunina and Babanin (1972)
50	37	Velikiy	Ukraine	Chernozem	—	450	49	19	30	Vadyunina and Babanin (1972)
47.4	42	Volgo	USSR	Kastanozem	—	450	50	15	35	Vadyunina and Babanin (1972)
47.4	42	Volgo	USSR	Kastanozem	—	450	33	15	18	Vadyunina and Babanin (1972)
52.7	41.5	Tambov	USSR	Chernozem	—	500	20	5	15	Vadyunina and Babanin (1972)
55.8	37.7	Moscow	USSR	Greyzem	—	550	26	10	16	Vadyunina and Babanin (1972)
51.8	36.2	Kursk	USSR	Chernozem	—	550	40	1	39	Vadyunina and Babanin (1972)
45	42	Stavropol	USSR	Chernozem	—	700	45	21	24	Vadyunina and Babanin (1972)
45	42	Stavropol Uplands	USSR	Solonetz	Loess	190	22	18	4	Alekseev <i>et al.</i> (1989)
45	42	Stavropol Uplands	USSR	Kastanozem	Loess	410	50	18	32	Alekseev <i>et al.</i> (1989)
49	47	Elton Plain	USSR	Kastanozem	Loess	200	22	15	7	Alekseev (pers. comm., 1994)
50	47	N Elton Plain	USSR	Kastanozem	Loess	300	34	5	29	Alekseev (pers. comm., 1994)
50	48	NE Elton Plain	USSR	Kastanozem	Loess	300	22	14	8	Alekseev (pers. comm., 1994)
38	-122	Yolo, California	US	Fluvisol	Alluvium	435	145	130	15	Singer and Fine (1989)
38	-122	Millsbholm, California	US	Luvisol	Siltstone	500	45	10	35	Singer and Fine (1989)
36.9	-122.1	Santa Cruz, California	US	Luvisol	Terrace	635	140	10	130	Singer and Fine (1989)
37.2	-122.0	Los Gatos, California	US	Luvisol	Phyllite	875	350	100	250	Singer and Fine (1989)
38	-122	Red Vine, California	US	Luvisol	Alluvium	950	315	40	274	Singer and Fine (1989)
39.3	-123.7	Caspar, California	US	Acrisol/Nitosol	Terrace	1000	200	10	190	Singer and Fine (1989)
39.3	-123.7	Ferncreek, California	US	Acrisol/Nitosol	Terrace	1000	450	0	450	Singer and Fine (1989)
38	-122	Josephine, California	US	Luvisol	Sandstone	1140	600	80	520	Singer and Fine (1989)
38	-122	Masteron, California	US	Cambisol	Schist	1500	500	0	500	Singer and Fine (1989)
36.0	-111.5	Painted Desert, Color.	US	—	—	250	4	2	2	Maher (1984)
35.8	-109.2	Navajo, Arizona	US	—	Sediment	300	28	3	25	Maher (1984)
37.3	-108.5	Mesa Verde, N. Mexico	US	—	Sandstone	350	19	3	16	Maher (1984)
37.3	-108.5	Mesa Verde, N. Mexico	US	—	Sandstone	350	31	4	27	Maher (1984)
39.2	-101.0	Colby, Kansas	US	—	Sediment	500	185	36	149	Maher (1984)
36.5	-105.3	Ranchos de T., N. Mex.	US	—	—	700	167	5	162	Maher (1984)
37.7	-119.5	Yosemite, California	US	—	Granite	1000	168	28	140	Maher (1984)
37.8	-080.9	White Sulph. Spr, W. Virg	US	—	—	1100	127	8	119	Maher (1984)
33.4	4.9	Dayat Iffir, Mid Atlas	Morocco	—	Dolomite	666	21	1	20	Maxted (1989)
32.9	5.4	Tigalmamine M. Atlas	Morocco	—	Dolomite	918	35	1	34	Maxted (1989)
48	11.5	Bavaria	Germany	Cambisol	Loess	800	45	13	32	Fassbinder (1994)
50.7	-3.5	Jackmoor Brook	England	Cambisol	Red Beds	800	250	10	240	Maher (1984)
50.7	-3.5	Jackmoor Brook	England	Cambisol	Red Beds	800	210	10	200	Oldfield <i>et al.</i> (1979)
35	32.5	Kissonerga	W Cyprus	—	Marl	600	80	5	75	Tipping and Peters (1995)
41	16	S Apennines	Italy	—	Limestone	700	400	-0	400	Tite and Linington (1986)
43	12	C Apennines	Italy	—	Limestone	1000	300	-0	300	Tite and Linington (1986)

area. The results of our magnetic susceptibility approach to paleorainfall reconstructions indicate increased precipitation, due to more intense summer monsoonal activity, in the early Holocene and during the last interglaciation. These increases are on the order of +25 to 80% (compared to the present day) for the presently semiarid western area, and +5 to 25% for the more humid south and east. In contrast, during glaciations, we identify decreased rainfall across the Loess Plateau of up to ~50% (Figs. 3 and 4). The paleoisohyet maps shown in Fig. 4 illustrate the more northerly penetration of the moisture-bearing summer monsoonal winds during the early Holocene and last interglaciation. These results match well with independent indicators of paleoprecipitation, such as pollen evidence (Jarvis, 1993), general circulation modeling (Kutzbach and Guetter, 1988), soil particle size analysis (Banerjee *et al.*, 1993), and lake levels (Wang, 1983).

We can extend our rainfall reconstructions to the last 1.1 myr, using the long susceptibility record from Xifeng, in the central part of the Loess Plateau (Fig. 1b). The susceptibility data of Liu *et al.* (1992) were log-transformed, scaled, and matched to the ocean core $\delta^{18}\text{O}$ record (Site 677) of Raymo *et al.* (1990), using the sequence slotting approach of Thompson and Clark (1993). A good match was found between the $\delta^{18}\text{O}$ and scaled susceptibility back to isotope stage 33. The loess record lacks sufficient resolution to match to the $\delta^{18}\text{O}$ record beyond 1.1 myr. Matching the loess susceptibility record, by sequence slotting, with the orbitally tuned $\delta^{18}\text{O}$ record allows the loess sequence to be transformed from a depth to an age scale (Fig. 1b). Using the susceptibility/rainfall calibration

equation of Maher *et al.* (1994), we find variations in annual paleorainfall at this site from 300 mm or less during glaciations to ~700 mm during interglaciations. We identify the wettest periods to have been in isotope stages 5, 7, 11, and 13. The driest stage is stage 22, at ~800,000 yr. Over the last 1.1 myr, we find that for 80% of the time, rainfall at Xifeng was lower than the present day. Before ~700,000 yr ago, the amplitude of the susceptibility variations is significantly less than that in the later Pleistocene. It is possible that postdepositional diagenesis at depth in these sequences has attenuated the susceptibility record. However, the reduced scale of variation in the loess susceptibility record is reflected by a similar pattern in the deep-sea oxygen isotope record (Fig. 1a). One notable difference between the $\delta^{18}\text{O}$ and susceptibility data occurs at oxygen isotope stage 13, ~500,000 yr, when rainfall (\approx Asian paleomonsoon) was apparently particularly high (intense) but the $\delta^{18}\text{O}$ value (\approx global ice volume) for this period is not extreme. Additional loess data would be required to assess whether this difference is of local or regional significance.

PEDOGENIC SUSCEPTIBILITY AND TIME

In using pedogenic susceptibility values to reconstruct paleoclimate in this way, it is essential to determine if pedogenic susceptibility is a rapidly formed soil property. In contrast to our approach, Heller *et al.* (1993) assume that susceptibility development in the Chinese loess and soil sequences develops linearly with time, and hence they use age models to calculate sediment accumulation rates and susceptibility *fluxes*. Their

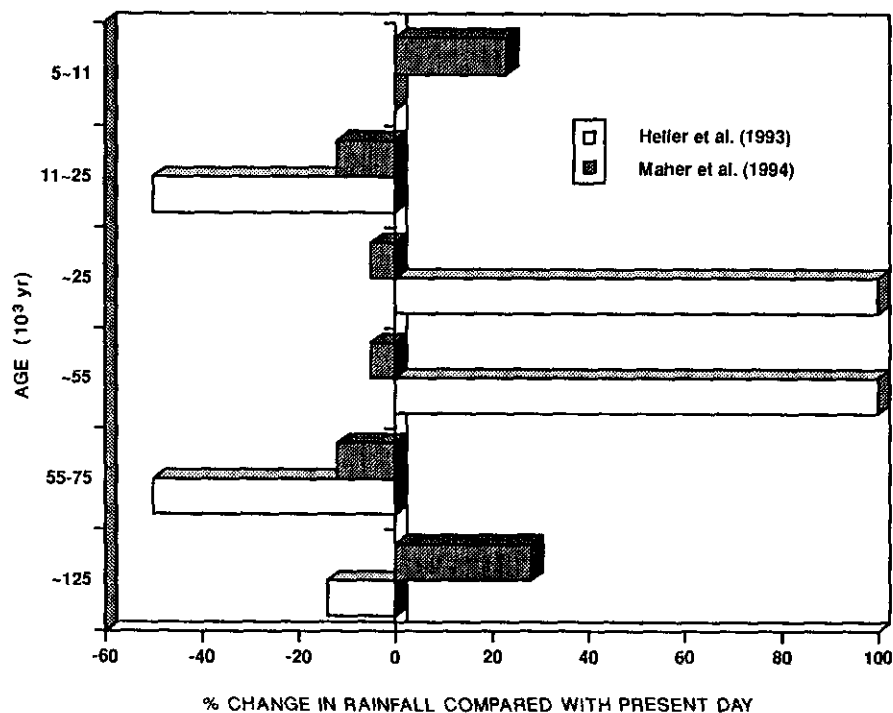


FIG. 3. Rainfall reconstructions (expressed as percent change from present-day rainfall) for the last glacial/interglacial cycle for Luochuan (from Heller *et al.*, 1993 and Maher *et al.*, 1994).

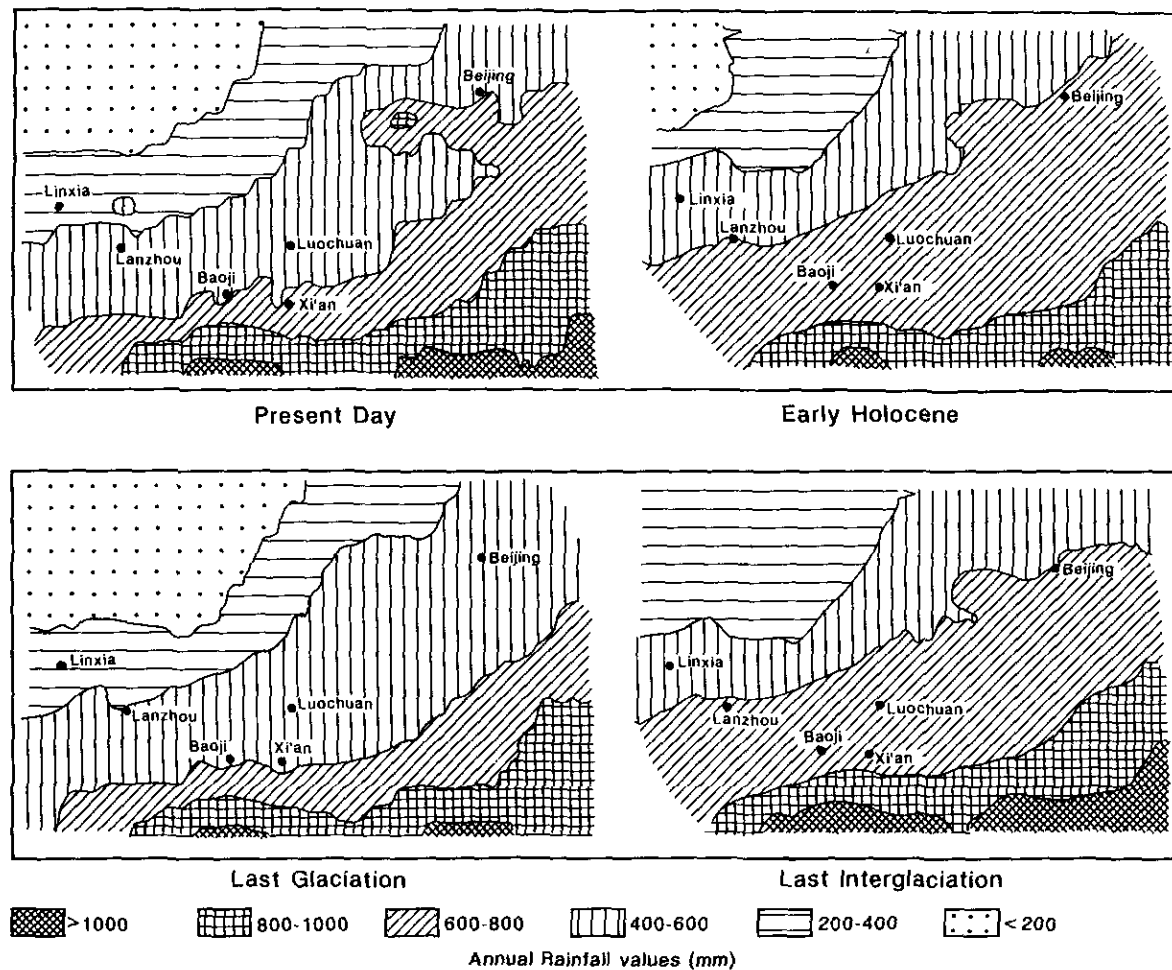


FIG. 4. Paleoisohyet maps for the Chinese Loess Plateau for the last glacial/interglacial cycle.

rainfall reconstructions strongly reflect variations in accumulation rate and are thus very different from our reconstructed values (Fig. 3).

Rates of soil formation on loess parent materials may be particularly rapid; Hallberg *et al.* (1978), for example, describe the formation of a soil from loess spoil material during just the last 100 yr. In this short span of time, a 31-cm A horizon has developed, the organic carbon content reached 2.6%, and translocation and accumulation of clay and silt occurred. Evidence for rapid development of pedogenic susceptibility comes from the Holocene Chinese loess soils used in our rainfall/susceptibility calibration (Maher *et al.*, 1994). The pedogenic susceptibility values of these young soils, which have developed on recent geomorphic surfaces, are in the same range as those of the buried paleosols, some of which have undergone much longer periods of pedogenesis. Such close similarities between the susceptibility of the young soils and the long-weathered paleosols would not be found if susceptibility were a slowly developing soil property. Furthermore, the susceptibility values of these young soils vary significantly from west to south and east, along the present-day gradient in precipitation (~350 mm in the west, ~700 mm in the south). Analysis of

the relationship between pedogenic susceptibility of the young soils and present-day climate variables identifies a weaker positive correlation with temperature, but predominantly a strong positive correlation with annual precipitation (Maher *et al.*, 1994).

All these observations could be explained if the susceptibility of these young soils has developed rapidly, to reach near-equilibrium with ambient climatic conditions. To test this hypothesis, we can extend examination of the pedogenic susceptibility/rainfall relationship on the Chinese Loess Plateau to other geographical areas in the Northern Hemisphere temperate zone (Fig. 5 and Table 1). Figure 6 plots pedogenic susceptibility against annual rainfall for all the sites in Table 1. We calculate pedogenic susceptibility by subtracting the susceptibility of the parent material from the maximum susceptibility value of the B horizon. As can be seen from Figure 7, pedogenic enhancement of susceptibility extends well into the B horizon of a soil. We do not use the A horizon value, which may be prone to surface pollution or burning effects (see below). Notwithstanding the scatter observable in the plot of pedogenic susceptibility against rainfall, there is a clear relationship between the two factors, susceptibility rising to a peak

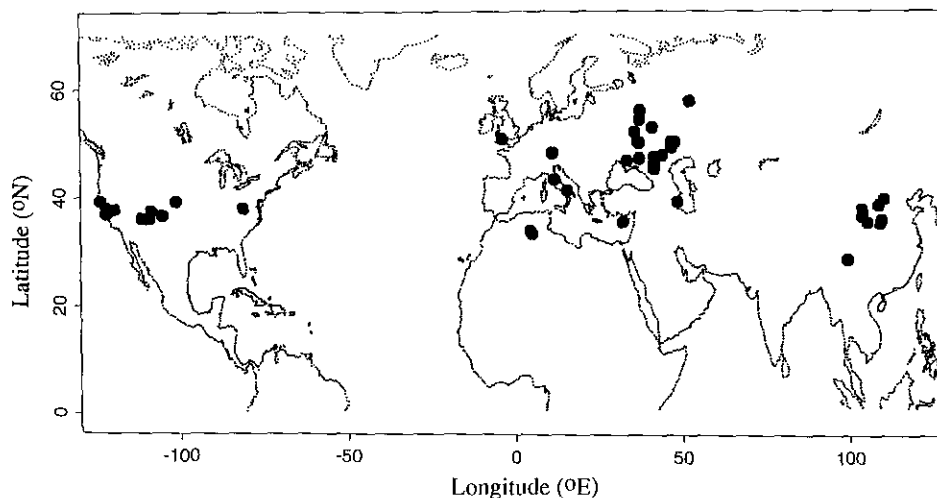


FIG. 5. Locations of soil sample sites, Northern Hemisphere temperate zone.

at around 1500 mm annual rainfall and probably falling under extremely high rainfall (3000 mm), as iron reduction dominates.

If we were to design the optimal soil sampling regime to test the susceptibility/rainfall relationship, we would deliberately exclude all of the following:

- (a) burnt soils (as burning efficiently enhances soil susceptibility);
- (b) poorly drained soils (as iron reduction generally counters the formation of ultrafine ferrimagnetic grains);
- (c) acidic soils (as pH below around 6.5 is unfavorable to precipitation of magnetite (Taylor *et al.*, 1988) and is also inhospitable to bacterial activity);

(d) eroded soils (which have lost their magnetically enhanced upper layers);

(e) tephra-containing or polluted soils (with extraneous additions to their ferrimagnetic content);

(f) strongly ferrimagnetic parent materials (e.g., basic igneous rocks), whose "inherited" properties dominate the soil susceptibility; and

(g) slowly weathering or iron-deficient parent materials (e.g., quartzose sands).

Given that the data in Figure 6, our own data, and published data were obtained from a "less-than-optimal" sampling strategy, at least some of the scatter may be related to points a–g above. Nevertheless, it seems unlikely that the overall corre-

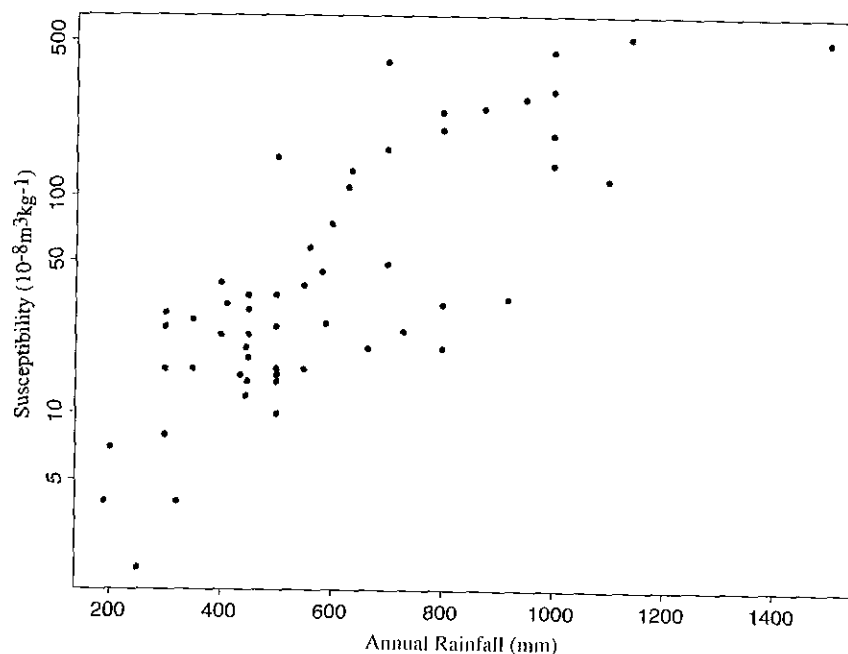


FIG. 6. Pedogenic susceptibility versus annual rainfall, based on data from Table 1.

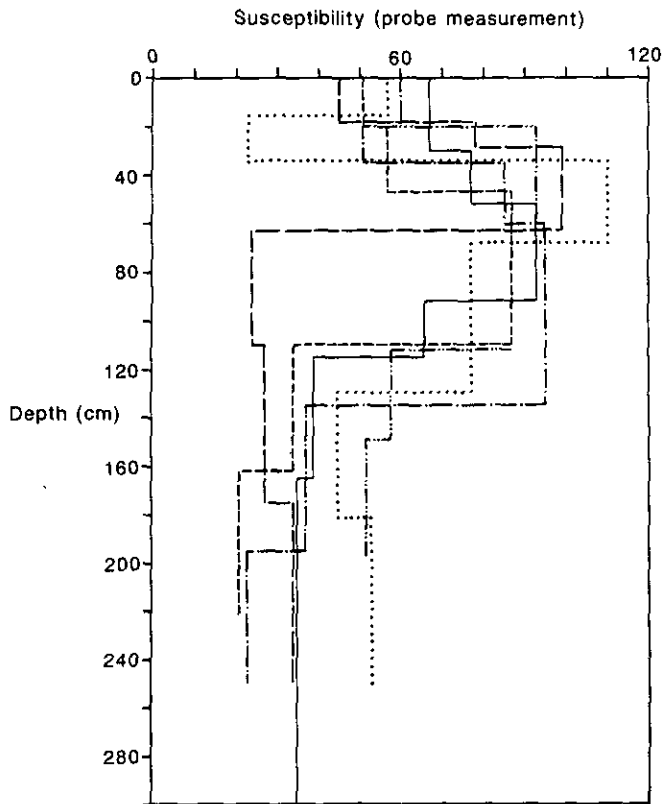


FIG. 7. Volume susceptibility measurements for modern soils on the Chinese Loess Plateau. Note that the apparent decreases in susceptibility values in the topsoil are due to decreasing soil density. (From Maher et al., 1994)

lation is due to chance. It would be difficult to envisage such a relationship between pedogenic susceptibility and rainfall if weathering duration was a more dominant factor than climate. The Northern Hemisphere temperate zone data set also allows us to assess the importance of temperature for susceptibility enhancement. We find (Table 2) a weak but statistically significant positive correlation between winter temperature and susceptibility enhancement. However, annual rainfall is the dominant explanatory variable. In contrast, Singer *et al.* (1992), on the basis of chronosequence studies on Californian soils, propose an hypothesis that is directly opposite to the one described here. They identify a linear increase in pedogenic susceptibility with time. Some of the Californian soils on younger tectonic surfaces appear, according to our hypothesis,

TABLE 2
Northern Hemisphere Pedogenic Susceptibility vs Climate
Correlation Matrix

	Rainfall	Winter temp.	Mean temp.	Summer temp.
Log [Susceptibility (B-C)]	0.81 (0.000)	0.57 (0.000)	0.37 (0.005)	-0.28 (0.042)
Susceptibility (B-C)	0.78 (0.000)	0.55 (0.000)	0.35 (0.009)	-0.28 (0.038)

Note. Numbers in brackets are *p* values; degrees of freedom = 53.

to be "under-enhanced" for the rainfall they receive. Hence, assuming these soils have not been eroded and that the time controls ascribed are accurate, the duration of weathering appears to have been insufficient for the prerequisite of our hypothesis, namely that near-steady state values of pedogenic susceptibility have been achieved. As indicated by the list of exclusions above, magnetic enhancement can be retarded under unfavorable soil-forming conditions, such as a poorly buffered soil environment.

The validity of our susceptibility/rainfall hypothesis can be tested by further magnetic studies of both modern-day soils and well-dated soil chronosequences. Given the unique and detailed record of paleoclimate preserved by the Chinese loess sequences, and the scarcity of records of paleoprecipitation, testing and validation or refutation of this hypothesis is an important step in quantitative reconstruction of paleoclimate from these proxy records.

ACKNOWLEDGMENTS

We are very grateful to Julii Brainard for providing the GIS-generated paleoisohyet maps and Friedrich Heller for kindly providing susceptibility data from the long Xifeng loess sequence.

REFERENCES

- Alekseev, A. O., Kovalevskaya, I. S., Morgun, Ye. G., and Samovlova, Y. M. (1989). Magnetic susceptibility of soils in a catena. *Soviet Soil Science* 21(1), 78-86.
- Evans, M. E., and Heller, F. (1994). Magnetic enhancement and palaeoclimate: Study of a loess/palaeosol couplet across the loess plateau of China. *Geophysical Journal International* 117, 257-264.
- Fassbinder, J. (1992). Naturwissenschaftliche untersuchungen an boenbackterien: neuentdeckte grundlagen fur die magnetische prospektion archaologischer denkmaler in Bayern. *Das Archaologische Jahr in Bayern* 1991, 211-215.
- Hallberg, G. R., Wollenhaupt, N. C., and Miller, G. A. (1978). A century of soil development in spoil derived from loess in Iowa. *Soil Science Society of America Journal* 42, 339-343.
- Heller, F., and Liu, T.-S. (1986). Palaeoclimatic and sedimentary history from magnetic susceptibility of loess in China. *Geophysical Research Letters* 13, 1169-1172.
- Heller, F., Shen, C.-D., Beer, J., Liu, X.-M., Liu, T.-S., Bronger, A., Suter, M., and Bonani, G. (1993). Quantitative estimates of pedogenic ferromagnetic mineral formation in Chinese loess and palaeoclimatic implications. *Earth and Planetary Science Letters* 114, 385-390.
- Jarvis, D. I. (1993). Pollen evidence of changing Holocene monsoon climate in Sichuan Province, China. *Quaternary Research* 39, 325-337.
- Kutzbach, J. E., and Guetter, P. J. (1988). The influence of changing orbital parameters and surface boundary conditions on climate simulations for the past 18,000 years. *Journal of Atmospheric Science* 43, 1726-1759.
- Liu, X. M., Shaw, J., Liu, T., Heller, F., and Yaun, B. (1992). Magnetic mineralogy of Chinese loess and its significance. *Geophysical Journal International* 108, 301-308.
- Lovley, D. R., Stolz, J. F., Nord, G. L., and Phillips, E. J. P. (1987). Anaerobic production of magnetite by a dissimilatory iron-reducing microorganism. *Nature* 330, 252-254.
- Lukshin, A. A., Rumyantseva, T. I., and Kovrigo, V. P. (1968). Magnetic sus-

- ceptibility of the principal soil types of the Udmurt Assr. *Soviet Soil Science* **3**, 88–93.
- Maher, B. A. (1984). "Origins and Transformation of Magnetic Minerals in Soils." Ph.D. thesis, University of Liverpool.
- Maher, B. A., and Thompson, R. (1991). Mineral magnetic record of the Chinese loess and paleosols. *Geology* **19**, 3–6.
- Maher, B. A., and Thompson, R. (1992). Palaeoclimatic significance of the mineral magnetic record of the Chinese loess and paleosols. *Quaternary Research* **37**, 155–170.
- Maher, B. A., Thompson, R., and Zhou, L.-P. (1994). Spatial and temporal reconstructions of changes in the Asian palaeomonsoon: A new mineral magnetic approach. *Earth and Planetary Science Letters* **125**, 462–471.
- Maxted, R. W. (1989). Magnetic mineralogy and sediment yield of lake catchments in the Middle Atlas, Morocco. Ph.D. thesis, University of Wales.
- Oldfield, F., Rummery, T. A., Thompson, D. E., and Walling, D. E. (1979). Identification of suspended sediment sources by means of magnetic measurements: some preliminary results. *Water Resources Research* **15**(2), 211–218.
- Pavich, M. J., Brown, L., Harden, J., Klein, J., and Middleton, R. (1986). Be¹⁰ distribution in soils from Merced river terraces, California. *Geochemica Cosmochemica* **50**, 1727–1735.
- Raymo, M. E., Ruddiman, W. F., Shackleton, N. J., and Oppo, D. W. (1990). Evolution of Atlantic–Pacific $\delta^{13}\text{C}$ gradients over the last 2.5 m.v. *Earth and Planetary Science Letters* **97**, 353–368.
- Singer, M. J., and Fine, P. (1989). Pedogenic factors affecting magnetic susceptibility of Northern California soils. *Soil Science Society of America Journal* **53**, 1119–1127.
- Singer, M. J., Fine, P., Verosub, K. L., and Chadwick, O. A. (1992). Time dependence of magnetic susceptibility of soil chronosequences on the California coast. *Quaternary Research* **37**, 323–332.
- Taylor, R. M., Maher, B. A., and Self, P. G. (1987). Magnetite in soils: I. The synthesis of single-domain and superparamagnetic magnetite. *Clay Minerals* **22**, 411–422.
- Thompson, R., and Clark, R. M. (1993). Quantitative marine sediment core matching using a modified sequence-slotting algorithm. In "Journal of the Geological Society of London Special Publication 70, High Resolution Stratigraphy" (E. A. Hailwood and R. B. Kidd, Eds.), pp. 39–49.
- Tiedemann, R., and Sarnthein, M. (1994). Astronomic timescale for the Pliocene Atlantic $\delta^{18}\text{O}$ and dust flux records of Ocean Drilling Program site 659. *Paleoceanography* **9**(4), 619–638.
- Tipping, R., and Peters, C. (1995). (In press). "Sedimentological characteristics of samples from Kissonerga-Mosphillia, Cyprus." Edinburgh University Archeology Department Monograph.
- Tite, M. S., and Linington, R. E. (1986). The magnetic susceptibility of soils from central and southern Italy. *Estratto da Prospezioni Archeologiche* **10**, 25–36.
- Vadyunina, A. F., and Babanin, V. F. (1972). Magnetic susceptibility of some soils of the USSR. *Pochvovedeniye* **10**.
- Vadyunina, A. F., and Smirnov, Yu. A. (1978). Use of magnetic susceptibility for the study and mapping of soils. *Pochvovedeniye* **7**.
- Vandenberghe, R. E., De Grave, E., Hus, J. J., and Han, J.-M. (1992). Characterization of Chinese loess and associated palaeosol by Mössbauer spectroscopy. *Hyperfine Interactions* **70**, 977–980.
- Wang, Q.-M. (1983). Extension and retraction of Beiyangdian Lake in the past 10,000 years. *Geographical Research* **2**, 15–20.